Analysis of Structural Parameters for a Multi-Row Inclined Side Hole Muzzle Brake in an Airplane Gun

Ming Qiu, Hao Xie *, Yuxiang Tao, Zilong Deng, Jie Song

School of Mechanical Engineering, Nanjing University of Science and Technology, Nanjing, Jiangsu, 210094, China

* Corresponding Author Email: xiehao19970001@163.com

Abstract. In response to the low efficiency of a muzzle brake for a certain 30 mm airplane gun, a new type of muzzle brake with side ports tilted towards the rear of the barrel is proposed. Taking the flow state of the internal gas at the moment the projectile reaches the muzzle as the initial condition, a dynamic mesh method combining polyhedral stationary region and hexahedral structured mesh moving region is used to perform three-dimensional numerical simulation of the muzzle brake flow field considering the motion of the projectile. The influence of the number of side port rows and the angle of inclination of the side ports on the brake efficiency is analyzed. The results show that within a certain range, the brake efficiency increases with the increase in the number of side ports, but the increment gradually narrows. When the number of side port rows is 6, the brake efficiency can be increased to 42.3%. With the increase of the side hole inclination Angle, the braking efficiency increases first and then decreases. The optimal angle for this muzzle brake is between 115 degrees and 135 degrees. This study provides a reference for accurate efficiency calculation, design, and optimization of the new multi-row inclined side port muzzle brake.

Keywords: Muzzle brake, Multi-Row inclined side hole, Muzzle field, Control variable, Structural analysis.

1. Introduction

The muzzle brake is an aerodynamic device installed at the muzzle of a weapon, which reduces the flow of propellant gases from the central bore and directs a portion of the gases to flow out through side holes, thereby reducing the recoil impulse of the weapon. Muzzle brakes are widely used as one of the most effective recoil-reducing devices due to their significant recoil reduction effect, simple structure, and easy installation [1]. However, there are prominent issues with the current muzzle brakes for 30 mm airplane guns, such as low recoil reduction efficiency and improper design of the bore channels, which result in excessive recoil impulse and difficulties in mounting the weapons on helicopters or aircraft [2]. Therefore, designing high-efficiency muzzle brakes and analyzing the influence of their structural parameters on the brake efficiency are of great significance for the airplane gun research.

Most muzzle brakes for airplane guns adopt a straight hole design, which can direct a portion of the propellant gases to reduce the total forward momentum of the weapon. However, they do not fully utilize this portion of propellant gases to further reduce the recoil impulse by directing them towards the rear of the barrel. Considering the development of the sparse-wave recoil reduction technology. It is effective to design a lateral rear nozzle on the barrel of the weapon, reducing the recoil impulse by using the reaction force of the gunpowder gas in the barrel [3]. In this paper, a new type of multi-row oblique side hole muzzle brake is proposed. By accelerating the vented propellant gases from the side holes the energy of the propellant gases is further utilized to reduce the recoil impulse.

Numerical simulation of the muzzle flow field based on Computational Fluid Dynamics technology has become an important method for studying muzzle brake efficiency. Jiang [4] simulated the axisymmetric muzzle flow field by using a two-dimensional structured grid and TVD scheme. Zhang [5] performed numerical simulations of the muzzle flow field of an open chamber muzzle brake by using three-dimensional unsteady Euler equations combined with the high-precision Roe scheme. Wang Shisong [6] conducted numerical simulations of the muzzle flow field by using structural dynamic mesh technology based on two-dimensional unsteady Euler equations. Liu

Xinning [7] considered the motion of the projectile and used structured dynamic mesh simulation to model the projectile motion and perform three-dimensional numerical simulations of the muzzle flow field.

In order to study the impact of structural parameters on the brake, a numerical simulation of complex multi-row muzzle brake with oblique side holes is carried out. The three-dimensional N-S equation is used to obtain the flow state of gunpowder gas through each row of inclined side holes when the projectile moves, revealing the interaction mechanism between the projectile movement, the central bullet hole and the powder gas which flows in the inclined side hole, analyzing the influence law of the row number and the Angle of side holes on the brake efficiency, so as to provide a reference for the design of the new type of muzzle brake.

2. Design of multi-row oblique side hole muzzle brake

Most muzzle brakes for airplane guns were designed with a straight hole and did not fully utilize the propellant gases to further reduce the recoil impulse by directing them towards the rear of the barrel. Taking reference from the sparse wave recoil reduction technique, a new type of multi-row oblique side hole muzzle brake is proposed in this paper. By accelerating the vented propellant gases from the side holes towards the rear of the barrel when they pass through the muzzle, the energy of the propellant gases is further utilized to reduce the recoil impulse. The three-dimensional model of the multi-row oblique side hole muzzle brake is shown in Fig. 1, with a total of 5 rows and 2 columns of symmetrically designed oblique side holes. The inclination angle of the oblique side holes is 145 degrees, and the cross-sectional area is 432 mm2.

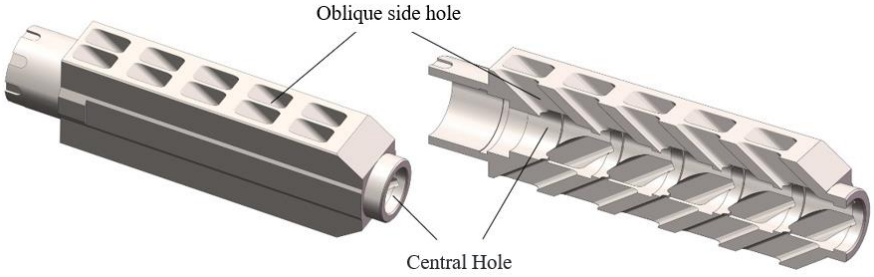

Figure 1. Three-dimensional model of the muzzle brake

3. Three-dimensional flow field numerical simulation

3.1. Three-dimensional flow field grid partitioning

Considering the symmetry of muzzle brake, 1/4 of the muzzle brake is taken as the study object for analysis. Based on the airplane gun measured 30 mm in length, a cylindrical region with a diameter of 1000 mm and lengths of 1000 mm in front of the muzzle and 500 mm behind the muzzle is set as the external computational domain. The grid division of the three-dimensional flow field model is shown in Fig. 2.

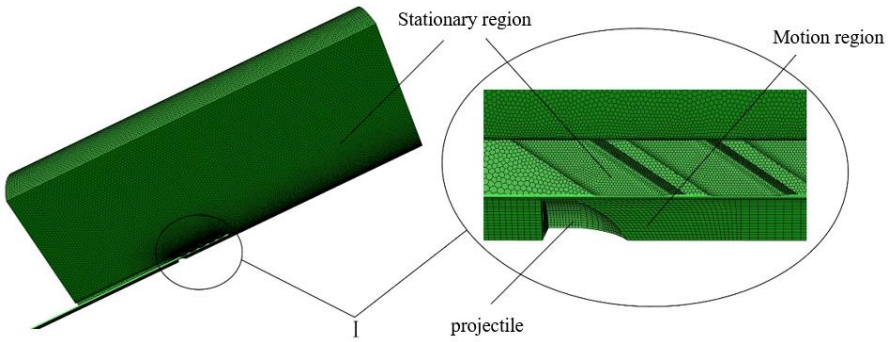

Figure 2. Computational domain meshing

In order to simulate the motion of projectile, the method of regional global motion processing divided by block grid is adopted. In order to improve the efficiency and accuracy of the calculation, the polyhedral meshes are divided into the static region of the fluid domain [8]. Due to the motion of the projectile, the fluid region before and after the projectile is changed, so it is treated as a moving region. The moving area is divided by hexahedral structured grid using the dynamic layering method in the moving grid technology. In the process of moving forward, the front grid of the projectile is disappearing and the rear grid is increasing. The data exchange between the moving region and the static region is realized by the numerical interpolation method through the interface. The mesh deformation caused by projectile motion will not affect the static region. For the boundary of the moving region and the static region, the numerical flux of the coincident part is obtained by the corresponding control bodies on both sides, and the non-coincident part is treated as the wall surface.

3.2. Three-dimensional flow field control equations

The gas phase of the propellant entering the muzzle brake the airflow outside the barrel can be treated as the same ideal gas, neglecting combustion and chemical reactions of the propellant. The three-dimensional Navier-Stokes equations for compressible viscous flow in a Cartesian coordinate system can be expressed as:

$$\partial\rho/\partial t + \partial(\rho u)/\partial x + \partial(\rho v)/\partial y + \partial(\rho w)/\partial z = 0 \tag{1}$$

$$\begin{cases} \partial(\rho u)/\partial t + \nabla\cdot(\rho u u) = -\nabla p + \mu\nabla^2 u + (\nabla\cdot\sigma)_x \\ \partial(\rho v)/\partial t + \nabla\cdot(\rho u v) = -\nabla p + \mu\nabla^2 v + (\nabla\cdot\sigma)_y \\ \partial(\rho w)/\partial t + \nabla\cdot(\rho u w) = -\nabla p + \mu\nabla^2 w + (\nabla\cdot\sigma)_z \end{cases} \tag{2}$$

$$\partial(\rho e)/\partial t + \nabla\cdot(\rho u e) = -\nabla\cdot(\rho u) + \nabla\cdot(k\nabla T) + (\nabla\cdot q) \tag{3}$$

ρ represents gas density; u, v, w are velocity components in the x, y, and z directions respectively; p is pressure; μ is dynamic viscosity; σ is stress tensor; k is thermal conductivity coefficient; T is temperature; q is heat flux vector; ∇ is gradient operator; ∇^2 is Laplacian operator; e represents total energy.

Control equations for layer-stacking grid:

$$h \geq (1+\alpha_s)h_{\text{ideal}} \tag{4}$$

$$h \leqslant \alpha_c h_{\text{ideal}} \tag{5}$$

The ideal height of a single unit grid is h_{ideal}; α_s is the segmentation factor for grid layers; α_c is the merging factor for grid layers. In the turbulence model established in this study, considering the actual size of the grid, α_s=0.4, α_c=0.2, h_{ideal}=3 mm.

3.3. Initial conditions and boundary conditions

For the initial time when the projectile reaches the muzzle brake, the calculation includes the motion of the projectile inside the muzzle brake and the entire post-muzzle brake period after ejection. The pressure, velocity, and temperature distribution of the gas in the barrel at the moment when the projectile reaches the muzzle brake are obtained from the calculation results of the two-phase flow ballistic model. These parameters are imported into the Fluent solver as initial conditions using user-defined functions.

The main boundary conditions include: Solid wall boundary conditions on the bottom of the barrel, the surface of the barrel, and the holes of the muzzle brake; Pressure outlet boundary conditions on the outer flow domain; Interface boundary conditions for data transfer between the stationary region and the dynamic region of the flow field, as well as symmetric plane boundary conditions. To ensure better convergence of the calculation, it is recommended to decrease the Courant number and relaxation factors appropriately. To improve the convergence of the calculation, it is recommended

to decrease the Courant number and relaxation factors appropriately. During the calculation, the axial force on the bottom of the barrel and the muzzle brake are monitored. At the beginning of the calculation, in order to simulate the flow field inside the muzzle brake more accurately, a time step of 10^{-6}s is used. The calculation continues until the end of the post-muzzle brake period.

3.4. Three-dimensional Flow Field Simulation Results

Starting from the moment the projectile reaches the recoil brake. The initial velocity of the projectile is obtained through the internal ballistics model. Fig. 3 shows the distribution of three-dimensional flow field pressure contours in the recoil brake at different times. From Fig. 3, it can be seen that after the high-temperature and high-pressure propellant gas enters the recoil brake with the projectile, it rapidly expands due to the increased space. Some propellant gas deviates outward along the axis of the barrel and enters the oblique side hole, where it undergoes significant compression after colliding with the outer wall of the oblique side hole. The airflow continues to deflect and accelerates outward along the oblique side hole, forming a supersonic airflow jet. There are vortex phenomena and obvious velocity boundary phenomena. Due to the obstruction effect of the bottom of the projectile, more propellant gas deviates and enters the oblique side hole, further compressing against the outer wall of the oblique side hole, gradually forming a strong conical oblique shock wave between the two symmetrical oblique side holes on the inner side of the central bore (Fig. 3(a)). The conical oblique shock wave hinders the airflow, which is conducive for more propellant to enter the oblique side hole. A conical oblique shock wave is formed between each group of oblique side holes. As the propellant gas passes through each conical oblique shock wave, the pressure decreases and the intensity of the conical oblique shock wave decreases sequentially (Fig. 3(b)). When the projectile passes through the fifth group of oblique side holes, there is no obvious strong shock wave formation. Overall, the external flow field of the muzzle brake has a conical distribution, and the pressure contour range which is formed at the mouth of the first group of oblique side holes is the widest, while the other groups of oblique side holes gradually weaken. This indicates that the most propellant gas is expelled from the first group of oblique side holes, and the expansion and acceleration of the airflow are also the most sufficient, resulting in the largest recoil impulse generated.

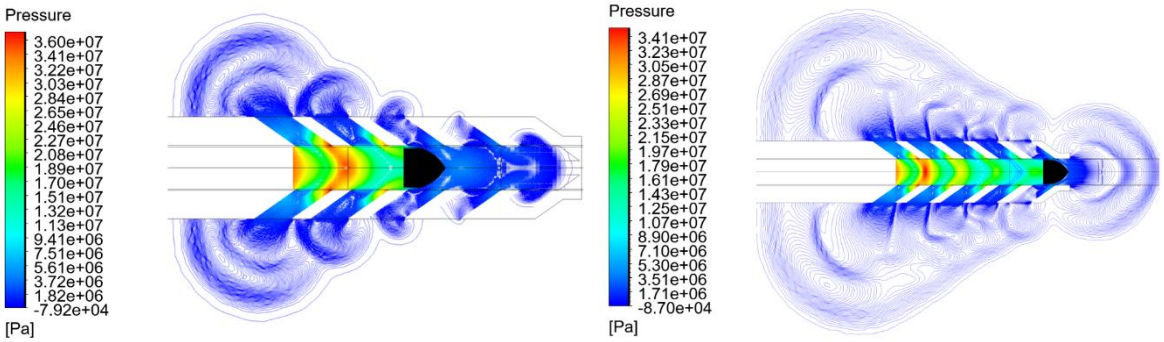

(a) t=0.1ms (b) t=0.2ms

Figure 3. Pressure contour distribution

4. Analysis of the main structural parameters' influence

There are many types of muzzle brakes, and they have various structural forms. However, they can be generally described as consisting of the following structural elements: the brake cavity, side ports, central bore hole, and the front wall of the brake chamber. Muzzle brakes typically have side ports, and the structural forms of these side ports vary. Some side ports have a small cross-sectional area and are angled with respect to the bore axis, while others have a large cross-sectional area, causing the side walls of the brake to take on a rib-like form. The efficiency of a muzzle brake is related to the ballistic conditions and structural dimensions of the brake, such as the diameter, length, cone angle of the brake cavity, inclination angle of the side ports, and caliber. In this study, two key

factors were selected for investigating their influence on the effectiveness of the muzzle brake: the number of side port rows and the angle of inclination of the side ports.

4.1. The influence of the number of side vent rows on the efficiency of a muzzle brake

By using the method of controlling variables, the number of side port rows of the muzzle brake was changed while keeping other structural parameters constant. Three-dimensional modeling of muzzle brakes with 4, 5, and 6 side port rows was performed, and Fluent was used to simulate the flow field for each case. The forces acting on the bottom of the bore and the muzzle brake were monitored. In the table, n represents the number of side port rows, α represents the angle of the side ports, S represents the area of the side ports, and ηz represents the recoil efficiency.

Based on the data results, the momentum efficiency [9] is used to evaluate the effectiveness of the muzzle brake. When the angle of the side ports is 145 degrees and the area of the side ports is 432 mm2, the impact of the number of side port rows on the recoil efficiency of the muzzle brake is as follows:

Table 1. The recoil efficiency of different side hole rows

n	α/deg	S/(mm^2)	η_z/%
4	145	432	33.6
5	145	432	38.4
6	145	432	42.3

From Table 1, it can be observed that the number of side vent rows has an impact on the effectiveness of the muzzle brake. When other conditions remain constant, increasing the number of side vent rows results in a greater amount of propellant gas being expelled through the side vent channels, leading to increased braking force and higher efficiency. However, there is a point where the incremental increase in efficiency becomes smaller after reaching a certain value. Additionally, increasing the number of side vent rows will also increase the length and mass of the muzzle brake, which may have some implications for the use of the firearm.

Fig. 4 shows a comparison of the braking forces experienced by muzzle brakes with different numbers of side vent rows. From the graph, it can be observed that the braking force remains relatively consistent as the propellant gas passes through the first four rows of side vents. When the gas passes through the fifth row of side vents, the braking force for both the muzzle brake with 5 rows and the one with 6 rows is also similar. In other words, increasing or decreasing the number of side vents does not significantly affect the forces acting on the earlier rows of side vents. However, an increase in the number of side vent rows leads to a higher peak value of the braking force, indicating a larger braking force efficiency. This trend holds true when other structural parameters remain unchanged.

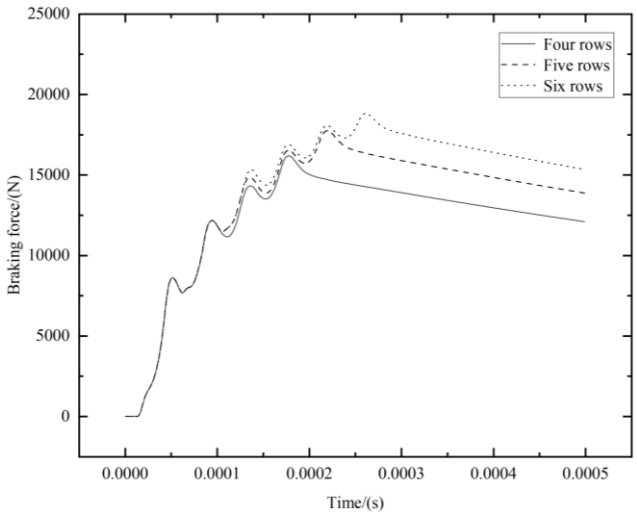

Figure 4. The braking force experienced by different numbers of side hole rows

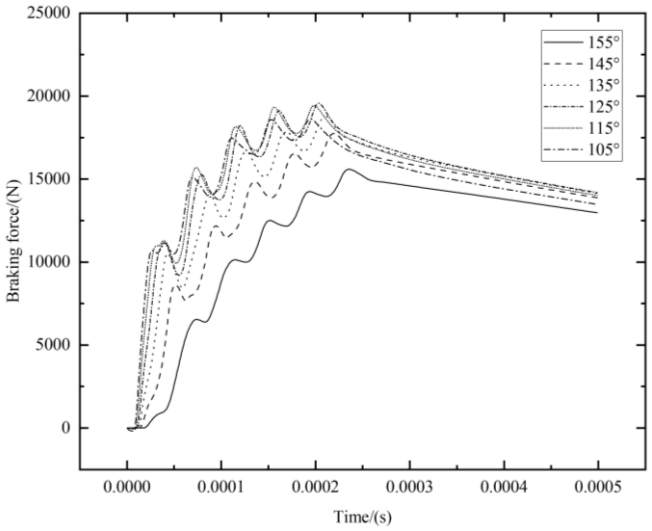

Figure 5. The braking force experienced by different side vent angles

4.2. The influence of the side vent angle on the effectiveness of the muzzle brake

By using the method of controlling variables, the angle of inclination of the side ports of the muzzle brake was changed while keeping the number of side ports, the area of the side ports, and other structural parameters constant. Three-dimensional modeling of the muzzle brake with side port angles of 105 degrees, 115 degrees, 125 degrees, 135 degrees, 145 degrees, and 155 degrees was performed. Fluent was used to simulate the flow field at the muzzle, and the forces acting on the bottom of the bore and each side port of the muzzle brake were monitored.

When the number of side holes is 5 rows and the area of side holes is 432 mm2, the Angle of side holes has the following effects on the withdrawal efficiency of the muzzle brake.

Table 2. The recoil efficiency of different side hole angles

n	α/deg	S/(mm^2)	η_z/%
5	105	432	38.6
5	115	432	39.5
5	125	432	39.9
5	135	432	39.4
5	145	432	38.4
5	155	432	35.6

From Table 2, it can be observed that the side vent angle of the muzzle brake has an impact on its effectiveness. Increasing the side vent angle leads to an increase in the effectiveness of the muzzle brake. In a certain range, the increase of side hole Angle will increase the brake efficiency. However, when the Angle of the side hole exceeds a certain value and continues to increase, the reduction efficiency becomes smaller. Because of that: as the increase of side vent angle α between the side vents and the axis of the bore, the axial component of the counterforce from the side vent airflow also increases, which improves the efficiency of the muzzle brake. However, if α becomes too large, the flow of gas entering the side vents will experience excessive turning, resulting in increased flow velocity loss and reduced flow rate through the side vents, leading to a decrease in efficiency. Therefore, to improve the effectiveness of the muzzle brake, it is not necessary to increase the side vent angle indefinitely, but rather there exists an optimal value. For this particular muzzle brake, the optimal side vent angle falls within the range of 115 degrees to 135 degrees.

Fig. 5 shows a comparison of the recoil forces experienced by muzzle brakes with different side port angles. From the figure, it can be observed that as the side port angle decreases, the peak value of the recoil force occurs more quickly when the propellant gas passes through the same side port. This is because, with the overall size of the muzzle brake remaining unchanged, a larger side port angle results in a longer side port, leading to slower gas ejection from the side port. The change in the

recoil force is not consistently correlated with the change in angle. During the process of decreasing the angle from 155 degrees to 125 degrees, the recoil force gradually increases. When the angle decreases from 135 degrees to 105 degrees, the change in the recoil force is relatively slow. At a side port angle of 125 degrees, the recoil efficiency reaches 39.9%.

5. Conclusion

A new type of multi-row inclined side port muzzle brake was proposed for a 30 mm airplane gun. Numerical simulations were conducted to analyze the three-dimensional transient flow state of the propellant gas when it passing through each row of inclined side ports. The results demonstrate that the inclined side ports can introduce high-pressure propellant gas into the bore and generate supersonic airflow spraying out from the rear, resulting in a significant reduction in recoil impulse and achieving the purpose of reducing weapon recoil. The muzzle brake also exhibits good compatibility with the airplane gun. By using the method of controlling variables, the effects of the number of side port rows and the angle of inclination of the side ports on the brake efficiency were analyzed. The results show that a higher number of side ports leads to a greater brake efficiency, but the incremental improvement becomes smaller after reaching a certain value. As the angle of inclination increases, the brake efficiency initially increases and then decreases. The optimal angle for this muzzle brake is between 115 degrees and 135 degrees.

Acknowledgements

This paper was supported by Basic scientific research projects of the State Administration of science, technology and industry for national defense (Grant No. JCKY2021209B016), and the National Natural Science Foundation of China (Grant No. 12072161and No. 51376090).

References

[1] Qiu M Song J. New principles and technologies for energy utilization of weapon propellant Gas [M]. Beijing: Defense Industry Press, 2022.12.

[2] Zha J.P. Numerical simulation of helicopter simulation bench under the action of aircraft gun shock wave [J]. Chinese Journal of Applied Mechanics, 2022, Vol.39 (4), p627-632.

[3] Qiu M, Guo F. Recoil reduction design of gas-controlled side-jet gun based on bifurcated two-phase flow model [J]. Journal of Mechanical Science and Technology, 2023, Vol.37(4), p1845-1857.

[4] Jiang Z, Chen Z. Numerical simulation of blast flow fields induced by a high-speed projectile [J]. Shock Waves, 2008, Vol.18 (3), p205-212.

[5] Zhang H, Chen Z. Investigations on the exterior flow field and the efficiency of the muzzle brake [J]. Journal of Mechanical Science and Technology, 2013, Vol.27 (1), p95-101.

[6] Wang S.S, Zheng J. Numerical simulation of muzzle flow field with muzzle brake [J]. Firepower and Command Control, 2011, Vol.36 (02), p148-151.

[7] Liu X.N, Yue M.K. Three-dimensional numerical simulation of muzzle flow field with muzzle brake for artillery [J]. Journal of Sichuan Ordnance, 2015, Vol.36 (07), p56-59.

[8] Hu K. ANSYS CFD engineering examples detailed explanation [M]. Beijing: People's Posts and Telecommunications Press, 2022, p16-40.

[9] Si P, Qiu M. Numerical simulation of two-phase flow considering piston recovery in lateral jet weapon [J]. Explosion and Shock, 2021, Vol.41 (08), p125-138.